EFFECTIVENESS OF THE DISTRIBUTION FACTOR APPROXIMATIONS USED IN CONGESTION MODELING

Minghai Liu
University of Illinois at Urbana Champaign
Illinois, U.S.A.
mliu@students.uiuc.edu

George Gross
University of Illinois at Urbana Champaign
Illinois, U.S.A.
gross@staff.uiuc.edu

Abstract – Congestion has widespread impacts on the availability and utilization of the existing transmission systems and consequently on the operation of competitive markets in electricity. The distribution factors play a key role in the modeling of congestion in various market applications. These factors are linear approximations of sensitivities of variables with respect to various inputs and are computed for a specified network topology and parameter values. In practice, the factors are used over a wide range of system conditions. This paper investigates the analytical characteristics, the robustness and the quality of the approximations provided by key distribution factors such as injection shift factors (*ISF*s) and power transfer distribution factors (*PTDF*s). We examine the range of conditions over which these factors can provide a reliable approximation for large power system networks. The numerical simulation results indicate that the errors of the approximations stay in an acceptable range under a broad spectrum of conditions including contingencies used to establish *n-1 security*.

Keywords: Distribution Factors, Injection Shift Factor (ISF), Power Transfer Distribution Factor (PTDF), Available Transfer Capability (ATC), Transmission Loading Relief (TLR), Congestion Modeling

1 INTRODUCTION

Open access of the transmission network has posed serious problems in the management of the transmission system. The congestion on the network becomes the main obstacle that, in great extend, impacts the operation and management of the power system. Critical information such as available transfer capability (*ATC*) [1], congestion relief schemes such as the transmission loading relief (*TLR*) procedure [2] and congestion management approaches such as incremental/decremental auctions and financial transmission rights (*FTR*/*FGR*) [3,4] are all impacted by the congestion situations on the grid. Solution of these problems requires explicit modeling of congestion.

Distribution factors play an essential role in congestion modeling. These distribution factors, including the injection shift factors (*ISF*s) and the power transfer distribution factors (*PTDF*s) have been widely used in the congestion modeling in many electricity market applications by providing fast approximations of the active power flow changes due to various system operations. These factors are basically linear approximations of the first order sensitivities of certain relationships in power systems computed for a specified network topology and parameter values. However, in many applications such as *ATC* evaluations and NERC's *TLR* procedures, distribution factors are considered to be constant in each time period even when the network parameters and topology are slightly different from those for which the distribution factors are computed [1,2]. This usage imposes questions on the robustness of the distribution factor applications. In fact, systematic studies of the behaviors of these distribution factors and the effectiveness of their applications in the congestion modeling have received scant attention so far.

This paper investigates the analytical characteristics, the effectiveness and robustness of approximations provided by key distribution factors such as *ISF*s and *PTDF*s. Starting with the actual derivation of these factors, we analyze their characteristics and examine the range of conditions over which these factors can provide a reliable approximation for large power system networks. In particular, we examine the effect of contingencies represented by changes in the network parameters and topology and investigate the robustness of the *PTDF* and *ISF* applications in congestion modeling. Numerical studies on various systems are provided to examine the robustness of the *ISF* and *PTDF* approximations for *ATC* information and *TLR* curtailments under a variety of loadings, system conditions and parameter values.

This paper consists of four additional sections. Section 2 reviews the definition and characteristics of the basic distribution factors. In section 3, the role of the distribution factors in the congestion modeling is illustrated by focusing on the evaluation of *ATC* and the deployment of NERC's *TLR* procedure. We devote section 4 to analyze the effects of the changes in the network parameters and topology and their impacts on the quality of distribution factor approximations. We summarize representative numerical results in section 4 to illustrate the robustness of the *ISF* and *PTDF* approximations in *ATC* evaluation and *TLR* curtailments determination.

2 BASIC DISTRIBUTION FACTORS

We consider a system with $N+1$ buses and L lines. We denote by $\mathcal{N} \triangleq \{0,1,2,\cdots,N\}$ the set of buses, with the slack bus at bus 0, and by $\mathcal{L} \triangleq \{\ell_1,\ell_2,\cdots,\ell_L\}$ the set of transmission lines and transformers that connect the

buses in the set $\mathcal{N}$. We denote each element $\ell \in \mathcal{L}$ by the *ordered* pair $\ell = (i, j)$ with the convention that the direction of the flow on line ℓ is from node *i* to node *j*. The serial admittance of line ℓ is $g_\ell - jb_\ell$, the active power flow is f_ℓ and $\underline{\boldsymbol{f}} \triangleq [f_1, f_2, \cdots, f_L]^T$. The net active power injection at node $n \in \mathcal{N}$ is denoted by p^n and we define $\underline{\boldsymbol{p}} \triangleq [p^1, p^2, \cdots, p^N]^T$. Transactions are represented by the set of power injection-withdrawal (*I-W*) node pairs, $\mathcal{W} \triangleq \{w_1, w_2, \cdots, w_W\}$, with each element in this set denoted by the *ordered* triplet $w = \{m, n, t\}$ representing an *I-W* node pair with *from* node *m*, *to* node *n*, in the amount *t*.

We study the response of the active line flow to changes in nodal injections. Consider the nodal injection vector $\underline{\boldsymbol{p}}$ and the corresponding active line flow vector $\underline{\boldsymbol{f}}$. Denote the system state by $\underline{\boldsymbol{s}} \triangleq \left[\underline{\boldsymbol{\theta}}^T, \underline{\boldsymbol{V}}^T\right]^T$, where $\underline{\boldsymbol{\theta}} \triangleq [\theta^1, \theta^2, \cdots, \theta^N]^T$ ($\underline{\boldsymbol{V}} \triangleq [V^1, V^2, \cdots, V^N]^T$) is the voltage phase angle (magnitude) vector. Denote the reference conditions by $\underline{\boldsymbol{p}}^{(0)}$, $\underline{\boldsymbol{s}}^{(0)}$ and $\underline{\boldsymbol{f}}^{(0)}$ that satisfy:

$$\begin{cases} \underline{\boldsymbol{g}}(\underline{\boldsymbol{s}}^{(0)}) - \underline{\boldsymbol{p}}^{(0)} = \underline{\boldsymbol{0}} & (1) \\ \underline{\boldsymbol{h}}(\underline{\boldsymbol{s}}^{(0)}) - \underline{\boldsymbol{f}}^{(0)} = \underline{\boldsymbol{0}} & (2) \end{cases}$$

where (1) represents a statement of the active power flow equations and the component ℓ of $\underline{\boldsymbol{h}}(\bullet)$,

$$h_\ell(\underline{\boldsymbol{s}}) = g_\ell\left[V^{i2} - V^i V^j \cos(\theta^i - \theta^j)\right] + b_\ell V^i V^j \sin(\theta^i - \theta^j) \quad (3)$$

is the expression for the active flow on line $\ell = (i, j), \ell \in \mathcal{L}$. For a small change $\underline{\Delta \boldsymbol{p}}$ that changes the value from $\underline{\boldsymbol{p}}^{(0)}$ to $\underline{\boldsymbol{p}}^{(0)} + \underline{\Delta \boldsymbol{p}}$, we denote by $\underline{\Delta \boldsymbol{s}}$ ($\underline{\Delta \boldsymbol{f}}$) the corresponding change in the state $\underline{\boldsymbol{s}}$ (active line flows $\underline{\boldsymbol{f}}$). We assume the system stays in balance for the change $\underline{\Delta \boldsymbol{p}}$ and neglect the changes in losses so that, for every *MW* increase in the injection at node $n \neq 0$, there is a corresponding *MW* increase in the withdrawal at the slack node *0*. In other words, $\Delta p^0 = -\sum_{n \in \mathcal{N}, n \neq 0} \Delta p^n$.

We apply the first order Taylor's series expansion near the reference point $\underline{\boldsymbol{s}}^{(0)}$:

$$\begin{cases} \underline{\boldsymbol{g}}(\underline{\boldsymbol{s}}^{(0)} + \underline{\Delta \boldsymbol{s}}) = \underline{\boldsymbol{g}}(\underline{\boldsymbol{s}}^{(0)}) + \left.\dfrac{\partial \underline{\boldsymbol{g}}}{\partial \underline{\boldsymbol{s}}}\right|_{\underline{\boldsymbol{s}}^{(0)}} \underline{\Delta \boldsymbol{s}} + h.o.t. & (4) \\ \underline{\boldsymbol{h}}(\underline{\boldsymbol{s}}^{(0)} + \underline{\Delta \boldsymbol{s}}) = \underline{\boldsymbol{h}}(\underline{\boldsymbol{s}}^{(0)}) + \left.\dfrac{\partial \underline{\boldsymbol{h}}}{\partial \underline{\boldsymbol{s}}}\right|_{\underline{\boldsymbol{s}}^{(0)}} \underline{\Delta \boldsymbol{s}} + h.o.t. & (5) \end{cases}$$

For "small" $\underline{\Delta \boldsymbol{p}}$, $\underline{\Delta \boldsymbol{s}}$ is "small" and so we neglect the higher order terms (*h.o.t.*). We furthermore assume $\partial \underline{\boldsymbol{g}} / \partial \underline{\boldsymbol{s}}\big|_{\underline{\boldsymbol{s}}^{(0)}}$ to be nonsingular and henceforth drop the bar in the notation so that:

$$\underline{\Delta \boldsymbol{s}} \approx \left[\partial \underline{\boldsymbol{g}} / \partial \underline{\boldsymbol{s}}\right]^{-1} \underline{\Delta \boldsymbol{p}} \quad (6)$$

$$\underline{\Delta \boldsymbol{f}} \approx \frac{\partial \underline{\boldsymbol{h}}}{\partial \underline{\boldsymbol{s}}} \underline{\Delta \boldsymbol{s}} = \frac{\partial \underline{\boldsymbol{h}}}{\partial \underline{\boldsymbol{s}}} \left[\frac{\partial \underline{\boldsymbol{g}}}{\partial \underline{\boldsymbol{s}}}\right]^{-1} \underline{\Delta \boldsymbol{p}} \quad (7)$$

The *sensitivity matrix* in (7) depends on $\underline{\boldsymbol{s}}^{(0)}$ and this dependence on the system operating point makes it less than practical for power system applications.

To simplify the computation of the sensitivity matrix, we next introduce the assumptions used in the derivation of DC power flow models and make use of the reduced nodal susceptance matrix [5], $\underline{\boldsymbol{B}} \triangleq \underline{\tilde{\boldsymbol{A}}}^T \underline{\boldsymbol{B}}' \underline{\tilde{\boldsymbol{A}}}$, where $\underline{\boldsymbol{B}}' \triangleq diag\left[b_1, b_2, \cdots, b_L\right]$ is the diagonal branch susceptance matrix and $\underline{\tilde{\boldsymbol{A}}} \triangleq \left[\underline{\tilde{\boldsymbol{a}}}_1, \underline{\tilde{\boldsymbol{a}}}_2, \cdots, \underline{\tilde{\boldsymbol{a}}}_L\right]^T$ is the branch-to-node incidence matrix with the row ℓ of the matrix: $\tilde{a}_\ell \triangleq [0 \cdots 0 \overset{i}{1} 0 \cdots 0 \overset{j}{-1} 0 \cdots 0]^T$. We assume $\underline{\boldsymbol{B}}$ to be nonsingular. Under these assumptions, $\underline{\boldsymbol{s}}$ reduces to $\underline{\boldsymbol{\theta}}$ and the expressions for the partial derivatives become $\partial \underline{\boldsymbol{g}} / \partial \underline{\boldsymbol{\theta}} \approx \underline{\boldsymbol{B}}$, $\partial h_\ell / \partial \underline{\boldsymbol{\theta}} \approx b_\ell \underline{\tilde{\boldsymbol{a}}}_\ell$. We furthermore define $\underline{\boldsymbol{A}} \triangleq \underline{\boldsymbol{B}}' \underline{\tilde{\boldsymbol{A}}}$ to be the "admittance weighted" branch-node incidence matrix, then

$$\underline{\Delta \boldsymbol{f}} \approx \underline{\boldsymbol{A}} \underline{\boldsymbol{B}}^{-1} \underline{\Delta \boldsymbol{p}} \triangleq \underline{\boldsymbol{\Psi}} \underline{\Delta \boldsymbol{p}} \quad (8)$$

We henceforth replace the approximation by the equality:

$$\underline{\Delta \boldsymbol{f}} = \underline{\boldsymbol{\Psi}} \underline{\Delta \boldsymbol{p}}. \quad (9)$$

The $L \times N$ matrix $\underline{\boldsymbol{\Psi}} \triangleq \underline{\boldsymbol{A}} \underline{\boldsymbol{B}}^{-1}$ is an approximation of the *sensitivity matrix* and is called the injection shift factor (*ISF*) matrix. Since $\underline{\boldsymbol{A}}$ and $\underline{\boldsymbol{B}}$ are solely determined by the network topology and the line parameters, $\underline{\boldsymbol{\Psi}}$ is independent of $\underline{\boldsymbol{s}}^{(0)}$. The *ISF* of a line $\ell \in \mathcal{L}$ with respect to a change in injection at node $n \in \mathcal{N}, n \neq 0$ is the element ψ_ℓ^n in row ℓ, column *n* of $\underline{\boldsymbol{\Psi}}$. Note that ψ_ℓ^n is defined implicitly under the assumption that there is a corresponding change Δp^0 in the injection at the slack node *0* with $\Delta p^0 = -\Delta p^n$. Therefore, the ISF is dependent on the slack bus. As the location of the slack bus changes, the values of the *ISF*s may change. The notion of the *ISF* may be extended to include the slack bus *0*. Since the injection and withdrawal buses are identical in this case, $\psi_\ell^0 \equiv 0$ for any $\ell \in \mathcal{L}$.

In many applications, the impacts of changes in the quantity of an *I-W* node pair on the active line flows are of interest. We may evaluate the change in the active flow on a line ℓ due to a change Δt in the transfer quantity of an *I-W* node pair $w = \{m, n, t\} \in \mathcal{W}$ with *ISF*s. This change is represented by setting $\Delta p^m = \Delta t = -\Delta p^n$. The corresponding active flow change on line ℓ is

$$\Delta f_\ell = \psi_\ell^m \Delta p^m + \psi_\ell^n \Delta p^n = (\psi_\ell^m - \psi_\ell^n) \Delta t. \quad (10)$$

The *ISF* difference term is called the power transfer distribution factor (*PTDF*) of line ℓ with respect to the *I-W* node pair $w \in \mathcal{W}$ [1] and is defined by

$$\varphi_\ell^{(w)} \triangleq \Delta f_\ell / \Delta t = \psi_\ell^m - \psi_\ell^n. \quad (11)$$

In this case, the compensation at the slack bus cancels out since $\Delta p^m - \Delta p^n = (\Delta p^m - \Delta p^0) - (\Delta p^n - \Delta p^0)$. As such, the *PTDF* is independent of the slack bus.

A line $\ell = (i, j)$ is radial if either $\mathcal{H}_i = \{\ell\}$ or $\mathcal{H}_j = \{\ell\}$, where $\mathcal{H}_i$ ($\mathcal{H}_j$) is the set of lines that connect to node *i* (*j*). For the radial line ℓ with $\mathcal{H}_i = \{\ell\}$, $i \neq 0$,

$$\psi_\ell^n = \begin{cases} 1 & \text{if } n = i \\ 0 & \text{otherwise} \end{cases} \tag{12}$$

since the only impact on line ℓ comes from the injection at node *i*. For any other line $\ell' \neq \ell$, the injection change at the terminal nodes *i* and *j* has the same impact,

$$\psi_{\ell'}^i = \psi_{\ell'}^j \qquad \forall \ell' \neq \ell . \tag{13}$$

3 APPLICATIONS TO CONGESTION MODELING

Congestion has widespread impacts on the availability and utilization of the existing transmission systems. Key problems in the electricity market including the determination of available transfer capability (*ATC*) [1], the implementation of the congestion management approaches and the definition of transmission rights [3,4], are all impacted by the congestion situations on the grid. The solution of these problems requires explicit modeling of congestion. The models used have in common the application of distribution factors. In this section, we discuss the role of the distribution factors in congestion modeling by focusing on two important areas: the evaluation of *ATC* and the deployment of NERC's *TLR* procedure.

The available transfer capability (*ATC*) provides a measure of the transfer capability remaining in the physical transmission network for further commercial activity over and above already committed uses [1]. *ATC* represents the maximum additional *MW* that can be transferred between two specific areas while meeting all the defined pre- and post-contingency system conditions. A key component for the evaluation of *ATC* is the so-called uncommitted transfer capability (*UTC*) which is the total transfer capability (*TTC*) minus the existing transmission commitments. The computation of the *ATC* from *UTC* is straightforward since

$$ATC = UTC - CBM - TRM \tag{14}$$

where *CBM* is the capacity benefit margin and *TRM* is the transmission reliability margin [1]. All the transfer capability quantities are defined with respect to a sending node/area and a receiving node/area.

The modeling of congestion is a key issue in the determination of *UTC*. We denote by $\underline{f}^{max}$ the maximum active line flow limits and by $\underline{f}^{(0)}$ the active line flow corresponding to the existing transmission commitments constituting the reference case. Without loss of generality, we assume that the *UTC* quantities are determined by the dominant flows [6]. We consider $UTC^{m,n}$, where *m* is the *from* node and *n* is the *to* node. We introduce an additional *I-W* node pair, $w = \{m, n, \Delta t\}$, to the system and evaluate the change Δf_ℓ in the active power flow on each line $\ell \in \mathcal{L}$ due to w. We wish to determine the maximum amount Δt that can be transferred without causing any congestion. This problem is formulated as:

$$\begin{aligned} &max \quad \Delta t \\ &s.t. \quad \Delta f_\ell = \varphi_\ell^{(w)} \Delta t \le f_\ell^{max} - f_\ell^{(0)} \quad \forall \ell \in \mathcal{L} \end{aligned}$$

where we explicitly use the *PTDF* representation of the active line flow change. The optimal value of Δt is then the *UTC* quantity from node *m* to node *n* and

$$UTC^{m,n} = \min_{\ell \in \mathcal{L},\, \varphi_\ell^{(w)} > 0} \left\{ \frac{f_\ell^{max} - f_\ell^{(0)}}{\varphi_\ell^{(w)}} \right\} \triangleq \frac{f_{\bar{\ell}}^{max} - f_{\bar{\ell}}^{(0)}}{\varphi_{\bar{\ell}}^{(w)}} \tag{15}$$

where $\bar{\ell}$ is a line whose active flow limit determines $UTC^{m,n}$ and is referred to as a binding constraint line.

Clearly, the *PTDF*s play a key role in the determination of *UTC*. In fact, the *PTDF* representation results in the straightforward computation of *UTC* since only one traversal of all the lines is required to compute $UTC^{m,n}$ for each pair of nodes *m* and *n*.

We next discuss the role of the *PTDF*s in the transmission loading relief (*TLR*) procedure. *TLR* is the protocol used by NERC to prevent insecure operation of the interconnected grid in the Eastern Interconnection. The *TLR* procedure is invoked whenever some present or future insecure situations are identified, such as those arising when some proposed future transaction(s) load the network beyond specified operating security limits. Of the five different levels associated with *TLR*, three involve the rearrangement of the transactions and two require the curtailment, in part or whole, of the transactions. Our focus is on the levels 3 or 5 that involve transaction curtailments [2].

We represent the limit violation by the active overload on a line ℓ denoted by

$$\delta f_\ell = f_\ell - f_\ell^{max} . \tag{16}$$

We partition the *I-W* node pairs into two groups: $\mathcal{W}^+ \triangleq \{w \in \mathcal{W} : \varphi_\ell^{(w)} > 0\}$ and $\mathcal{W}^- \triangleq \{w \in \mathcal{W} : \varphi_\ell^{(w)} \le 0\}$. Without loss of generality, we assume the set $\mathcal{W}^-$ does not impact the overflow and the overflow δf_ℓ may be allocated to each $w \in \mathcal{W}^+$ so that

$$\widetilde{\delta f}_\ell^{(w)} = \frac{\varphi_\ell^{(w)} t}{\sum_{w' \in \mathcal{W}^+} \varphi_\ell^{(w')} t'} \delta f_\ell \tag{17}$$

is considered to be the portion of overflow attributable to $w \in \mathcal{W}^+$ [6]. The corresponding transfer amount is:

$$\widetilde{\delta t}^{(w)} = \frac{\widetilde{\delta f}_\ell^{(w)}}{\varphi_\ell^{(w)}} = \frac{t}{\sum_{w' \in \mathcal{W}^+} \varphi_\ell^{(w')} t'} \delta f_\ell \tag{18}$$

To relieve the congestion, we may curtail each *I-W* node according to $\widetilde{\delta t}^{(w)}$. Since $\varphi_\ell^{(w)}$ are very small for many $w \in \mathcal{W}^+$, their contributions to the congestion relief, $\varphi_\ell^{(w)} \widetilde{\delta t}^{(w)}$, is small. Consequently, NERC defined the set $\hat{\mathcal{W}} = \{w \in \mathcal{W}^+ : \varphi_\ell^{(w)} \ge 0.05\}$ which excludes the *I-W* node pairs with *PTDF* less than 0.05. NERC used the allocation rule given by:

$$\delta f_\ell^{(w)} = \frac{\left(\varphi_\ell^{(w)}\right)^2 t}{\sum_{w' \in \hat{\mathcal{W}}} \left(\varphi_\ell^{(w)}\right)^2 t'} \delta f_\ell \tag{19}$$

to determine the overflow attributed to $w \in \hat{\mathcal{W}}$. Then the curtailment associated with each $w \in \hat{\mathcal{W}}$ is:

$$\delta t^{(w)} = \frac{\delta f_\ell^{(w)}}{\varphi_\ell^{(w)}} = \frac{\varphi_\ell^{(w)} t}{\sum_{w' \in \hat{\mathcal{W}}} \left(\varphi_\ell^{(w')}\right)^2 t'} \delta f_\ell \,. \tag{20}$$

4 IMPACT OF CHANGES IN NETWORK TOPOLOGY AND PARAMETER VALUES

The *ISF*s and *PTDF*s play a key role in congestion modeling used in the new competitive environment. Clearly, these factors are evaluated for a given topology and parameter values and an operating point that satisfies, to a greater or lesser extent, the assumptions cited in the previous section. However, in many cases of interest, there are changes in the network topology, parameter values and the operating point, while the *ISF*s and *PTDF*s are held constant in the applications in which they are used. Such usage, in effect, neglects the impacts of these changes. In this section, we evaluate the effect of these changes and their impacts on the quality of distribution factor approximations.

We first consider the impacts of changes in network parameters. Let us denote by $\hat{\mathcal{L}} \triangleq \left\{\hat{\ell}_1, \hat{\ell}_2, \cdots, \hat{\ell}_{\hat{L}}\right\} \subseteq \mathcal{L}$ the subset of lines whose parameters are changed. For each line $\hat{\ell} \in \hat{\mathcal{L}}$, its line susceptance is changed from $b_{\hat{\ell}}$ to $b_{\hat{\ell}} + \Delta b_{\hat{\ell}}$. Denote the analogues of the matrices $\underline{\boldsymbol{B}}'$ ($L \times L$), $\underline{\tilde{\boldsymbol{A}}}$ and $\underline{\boldsymbol{\Psi}}$ ($L \times N$) corresponding to the lines in $\hat{\mathcal{L}}$ by $\underline{\boldsymbol{B}}'_{\hat{\mathcal{L}}} \triangleq diag[b_{\hat{\ell}_1}, b_{\hat{\ell}_2}, \cdots, b_{\hat{\ell}_{\hat{L}}}]$ ($\hat{L} \times \hat{L}$), $\underline{\tilde{\boldsymbol{A}}}_{\hat{\mathcal{L}}} \triangleq [\underline{\tilde{\boldsymbol{a}}}_{\hat{\ell}_1}, \underline{\tilde{\boldsymbol{a}}}_{\hat{\ell}_2}, \cdots, \underline{\tilde{\boldsymbol{a}}}_{\hat{\ell}_{\hat{L}}}]^T$ and $\underline{\boldsymbol{\Psi}}_{\hat{\mathcal{L}}} \triangleq [\underline{\boldsymbol{\psi}}_{\hat{\ell}_1}, \underline{\boldsymbol{\psi}}_{\hat{\ell}_2}, \cdots, \underline{\boldsymbol{\psi}}_{\hat{\ell}_{\hat{L}}}]^T$ ($\hat{L} \times N$) where $\underline{\boldsymbol{\psi}}_\ell^T$ is row $\hat{\ell}$ of $\underline{\boldsymbol{\Psi}}$, the ISF matrix. Let $\underline{\Delta \boldsymbol{B}'}_{\hat{\mathcal{L}}} \triangleq diag[\Delta b_{\hat{\ell}_1}, \Delta b_{\hat{\ell}_2}, \cdots, \Delta b_{\hat{\ell}_{\hat{L}}}]$, $\Delta b_{\hat{\ell}} \neq 0, \forall \hat{\ell} \in \hat{\mathcal{L}}$. The changes in $\hat{\mathcal{L}}$ result in changing the $\underline{\boldsymbol{B}}$ matrix into $\underline{\boldsymbol{B}} + \underline{\tilde{\boldsymbol{A}}}_{\hat{\mathcal{L}}}^T \underline{\Delta \boldsymbol{B}'}_{\hat{\mathcal{L}}} \underline{\tilde{\boldsymbol{A}}}_{\hat{\mathcal{L}}}$. This, in turn, changes each row of the ISF matrix by:

$$\underline{\Delta \boldsymbol{\psi}}_\ell^T = \begin{cases} \frac{\Delta b_\ell}{b_\ell} \underline{\boldsymbol{\psi}}_\ell^T - \frac{b_\ell + \Delta b_\ell}{b_\ell} \underline{\boldsymbol{\psi}}_\ell^T \underline{\tilde{\boldsymbol{A}}}_{\hat{\mathcal{L}}}^T (\underline{\boldsymbol{B}}'_{\hat{\mathcal{L}}} \underline{\Delta \boldsymbol{B}}'^{-1}_{\hat{\mathcal{L}}} + \underline{\boldsymbol{\Psi}}_{\hat{\mathcal{L}}} \underline{\tilde{\boldsymbol{A}}}_{\hat{\mathcal{L}}}^T)^{-1} \underline{\boldsymbol{\Psi}}_{\hat{\mathcal{L}}} & \ell \in \hat{\mathcal{L}} \\ -\underline{\boldsymbol{\psi}}_\ell^T \underline{\tilde{\boldsymbol{A}}}_{\hat{\mathcal{L}}}^T (\underline{\boldsymbol{B}}'_{\hat{\mathcal{L}}} \underline{\Delta \boldsymbol{B}}'^{-1}_{\hat{\mathcal{L}}} + \underline{\boldsymbol{\Psi}}_{\hat{\mathcal{L}}} \underline{\tilde{\boldsymbol{A}}}_{\hat{\mathcal{L}}}^T)^{-1} \underline{\boldsymbol{\Psi}}_{\hat{\mathcal{L}}} & \ell \notin \hat{\mathcal{L}} \end{cases} \tag{21}$$

The derivation of (21) is straightforward using the Sherman-Morrison-Woodbury formula [8].

For $\ell \notin \hat{\mathcal{L}}$, the $\hat{L}$-dimensional row vector $\underline{\boldsymbol{\phi}}_{\ell,\hat{\mathcal{L}}}^T \triangleq -\underline{\boldsymbol{\psi}}_\ell^T \underline{\tilde{\boldsymbol{A}}}_{\hat{\mathcal{L}}}^T (\underline{\boldsymbol{B}}'_{\hat{\mathcal{L}}} \underline{\Delta \boldsymbol{B}}'^{-1}_{\hat{\mathcal{L}}} + \underline{\boldsymbol{\Psi}}_{\hat{\mathcal{L}}} \underline{\tilde{\boldsymbol{A}}}_{\hat{\mathcal{L}}}^T)^{-1}$ establishes the relationship between the pre-change active flows $\underline{\boldsymbol{f}}_{\hat{\mathcal{L}}} \triangleq [f_{\hat{\ell}_1}, f_{\hat{\ell}_2}, \cdots, f_{\hat{\ell}_{\hat{L}}}]^T$ and the change Δf_ℓ in the active flows on line $\ell \notin \hat{\mathcal{L}}$ due to the parameter changes with $\Delta f_\ell = \underline{\boldsymbol{\phi}}_{\ell,\hat{\mathcal{L}}}^T \underline{\boldsymbol{f}}_{\hat{\mathcal{L}}}$. Particularly, if $\hat{\mathcal{L}} = \{\hat{\ell} = (\hat{i}, \hat{j})\}$, then $\underline{\boldsymbol{\phi}}_{\ell,\hat{\ell}} = -\frac{\psi_\ell^{\hat{i}} - \psi_\ell^{\hat{j}}}{b_{\hat{\ell}} / \Delta b_{\hat{\ell}} + (\psi_{\hat{\ell}}^{\hat{i}} - \psi_{\hat{\ell}}^{\hat{j}})}$ is proportional to the quantity $\psi_\ell^{\hat{i}} - \psi_\ell^{\hat{j}}$. Note that if both $\underline{\boldsymbol{B}}$ and $\underline{\boldsymbol{B}} + \underline{\tilde{\boldsymbol{A}}}_{\hat{\mathcal{L}}}^T \underline{\Delta \boldsymbol{B}'}_{\hat{\mathcal{L}}} \underline{\tilde{\boldsymbol{A}}}_{\hat{\mathcal{L}}}$ are nonsingular, $\underline{\boldsymbol{B}}'_{\hat{\mathcal{L}}} \underline{\Delta \boldsymbol{B}'}^{-1}_{\hat{\mathcal{L}}} + \underline{\boldsymbol{\Psi}}_{\hat{\mathcal{L}}} \underline{\tilde{\boldsymbol{A}}}_{\hat{\mathcal{L}}}^T$ is invertible [8].

Network topology changes such as line outages and line additions may be considered as special cases of parameter changes. For example, for the outage of a line $\hat{\ell} = (\hat{i}, \hat{j})$, $\hat{\mathcal{L}} = \{\hat{\ell}\}$, $\underline{\tilde{\boldsymbol{A}}}_{\hat{\mathcal{L}}} = \underline{\tilde{\boldsymbol{a}}}_{\hat{\ell}}^T$ and $\Delta b_{\hat{\ell}} = -b_{\hat{\ell}}$, so that:

$$\underline{\Delta \boldsymbol{\psi}}_\ell^T = \begin{cases} -\underline{\boldsymbol{\psi}}_{\hat{\ell}}^T & if \;\; \ell = \hat{\ell} \\ \frac{\psi_\ell^{\hat{i}} - \psi_\ell^{\hat{j}}}{1 - (\psi_{\hat{\ell}}^{\hat{i}} - \psi_{\hat{\ell}}^{\hat{j}})} \underline{\boldsymbol{\psi}}_{\hat{\ell}}^T & otherwise \end{cases} \tag{22}$$

where the factor $\phi_{\ell,\hat{\ell}} = \frac{\psi_\ell^{\hat{i}} - \psi_\ell^{\hat{j}}}{1 - (\psi_{\hat{\ell}}^{\hat{i}} - \psi_{\hat{\ell}}^{\hat{j}})}$ is called line outage distribution factor [1] which establishes the relationship between the pre-outage active flow $f_{\hat{\ell}}$ on line $\hat{\ell}$ and the change Δf_ℓ on the active flows on line $\ell \neq \hat{\ell}$ due to the outage of line $\hat{\ell}$ with $\Delta f_\ell = \phi_{\ell,\hat{\ell}} f_{\hat{\ell}}$. Note that $\psi_{\hat{\ell}}^{\hat{i}} - \psi_{\hat{\ell}}^{\hat{j}} = 1$ only when $\{\ell\}$ is a cutset of the network [7]. In that case, the outage of line ℓ breaks the system into two separate subnetworks and the *ISF*s needs to be redefined for each subnetwork.

Another example is the addition of a line $\hat{\ell} = (\hat{i}, \hat{j})$. Two possible situations of interest are:

(*i*) $\hat{\ell}$ is a radial line with $\hat{i} \notin \mathcal{N}$ whose addition results in $\tilde{\mathcal{L}} = \mathcal{L} \cup \hat{\ell}$ and $\tilde{\mathcal{N}} = \mathcal{N} \cup \hat{i}$. We may apply (12), (13) to construct the augmented *ISF* matrix

$$\tilde{\underline{\boldsymbol{\Psi}}} = \begin{bmatrix} \underline{\boldsymbol{\Psi}} & \underline{\boldsymbol{\psi}}^{\hat{i}} \\ \underline{\boldsymbol{0}}^T & 1 \end{bmatrix} \tag{23}$$

where $\underline{\boldsymbol{\psi}}^{\hat{i}} = \underline{\boldsymbol{\psi}}^{\hat{j}}$, the column $\hat{j}$ of $\underline{\boldsymbol{\Psi}}$;

(ii) $\hat{\ell}$ is a new line with $\hat{i}, \hat{j} \in \mathcal{N}$ whose addition results in $\tilde{\mathcal{L}} = \mathcal{L} \cup \hat{\ell}$. We define a new *ISF* row vector $\tilde{\underline{\boldsymbol{\psi}}}_{\hat{\ell}}^T \triangleq \underline{\boldsymbol{a}}_{\hat{\ell}}^T \underline{\boldsymbol{B}} = b_{\hat{\ell}} \underline{\tilde{\boldsymbol{a}}}_{\hat{\ell}}^T \underline{\boldsymbol{B}}$ and construct the augmented $(L+1) \times N$ ISF matrix

$$\tilde{\underline{\boldsymbol{\Psi}}} = \begin{bmatrix} \underline{\boldsymbol{\Psi}} + \underline{\Delta \boldsymbol{\Psi}} \\ \tilde{\underline{\boldsymbol{\psi}}}_{\hat{\ell}}^T + \underline{\Delta \boldsymbol{\psi}}_{\hat{\ell}}^T \end{bmatrix} \tag{24}$$

where $\underline{\Delta \boldsymbol{\psi}}_{\hat{\ell}}^T$ and each row of $\underline{\Delta \boldsymbol{\Psi}}$ is determined by $\underline{\Delta \boldsymbol{\psi}}_\ell^T = -\frac{\psi_\ell^{\hat{i}} - \psi_\ell^{\hat{j}}}{1 + (\tilde{\psi}_{\hat{\ell}}^{\hat{i}} - \tilde{\psi}_{\hat{\ell}}^{\hat{j}})} \tilde{\underline{\boldsymbol{\psi}}}_{\hat{\ell}}^T$.

A change in the network topology or parameter values will change the *PTDF* values from those in the base case. However, industry practice typically does not update the values; instead, the base case values are kept. This practice, in turn, impacts the quality of the *PTDF* applications in congestion modeling. We investigate these impacts by evaluating the relative errors in the

calculation of *ATC* and *TLR* actions due to the neglect of the *PTDF* changes.

We first consider the *ATC* application. Denote by $\underline{\underline{\Psi}}$ and $\varphi_\ell^{(w)}$ the *ISF* matrix and the *PTDF* value of each line $\ell \in \mathcal{L}$ with respect to each *I-W* node pair $w \in \mathcal{W}$ for the modified (reference) network, respectively, and by $\underline{\underline{\Psi}} + \underline{\underline{\Delta\Psi}}$ and $\varphi_\ell^{(w)} + \Delta\varphi_\ell^{(w)}$ those that are used to evaluate $UTC^{m,n}$. From (15)

$$UTC^{m,n}\left(\underline{\underline{\Psi}}\right) = \min_{\varphi_\ell^{(w)}>0} \left\{ \frac{f_\ell^{max} - f_\ell^{(0)}}{\varphi_\ell^{(w)}} \right\} \triangleq \frac{f_{\bar{\ell}}^{max} - f_{\bar{\ell}}^{(0)}}{\varphi_{\bar{\ell}}^{(w)}}$$

$$UTC^{m,n}\left(\underline{\underline{\Psi}}+\underline{\underline{\Delta\Psi}}\right) = \min_{\varphi_\ell^{(w)}+\Delta\varphi_\ell^{(w)}>0} \left\{ \frac{f_\ell^{max} - f_\ell^{(0)}}{\varphi_\ell^{(w)}+\Delta\varphi_\ell^{(w)}} \right\} \triangleq \frac{f_{\bar{\bar{\ell}}}^{max} - f_{\bar{\bar{\ell}}}^{(0)}}{\varphi_{\bar{\bar{\ell}}}^{(w)}+\Delta\varphi_{\bar{\bar{\ell}}}^{(w)}}$$

It follows that $\dfrac{f_{\bar{\bar{\ell}}}^{max} - f_{\bar{\bar{\ell}}}^{(0)}}{\varphi_{\bar{\bar{\ell}}}^{(w)}+\Delta\varphi_{\bar{\bar{\ell}}}^{(w)}} \le \dfrac{f_{\bar{\ell}}^{max} - f_{\bar{\ell}}^{(0)}}{\varphi_{\bar{\ell}}^{(w)}+\Delta\varphi_{\bar{\ell}}^{(w)}}$ and

$$\frac{UTC^{m,n}\left(\underline{\underline{\Psi}}+\underline{\underline{\Delta\Psi}}\right) - UTC^{m,n}\left(\underline{\underline{\Psi}}\right)}{UTC^{m,n}\left(\underline{\underline{\Psi}}\right)} \le \frac{\varphi_{\bar{\ell}}^{(w)}}{\varphi_{\bar{\ell}}^{(w)}+\Delta\varphi_{\bar{\ell}}^{(w)}} - 1 \approx \frac{-\Delta\varphi_{\bar{\ell}}^{(w)}}{\varphi_{\bar{\ell}}^{(w)}}$$

The relative errors in the *UTC* are bounded by the relative errors in the *PTDF* of the binding constraint lines.

Next we investigate the impact of the errors in $\underline{\underline{\Psi}}$ on the curtailment quantity computation in the *TLR* procedure. We adopt the same notation and assume line ℓ is congested with the active overflow δf_ℓ. The curtailment quantities associated with each $w \in \hat{\mathcal{W}}$ in the two cases are determined by:

$$\delta t^{(w)}\left(\underline{\underline{\Psi}}\right) = \frac{\varphi_\ell^{(w)} t}{\sum_{w' \in \hat{\mathcal{W}}\left(\underline{\underline{\Psi}}\right)} \left(\varphi_\ell^{(w')}\right)^2 t'} \delta f_\ell$$

$$\delta t^{(w)}\left(\underline{\underline{\Psi}}+\underline{\underline{\Delta\Psi}}\right) = \frac{\left(\varphi_\ell^{(w)}+\Delta\varphi_\ell^{(w)}\right) t}{\sum_{w' \in \hat{\mathcal{W}}\left(\underline{\underline{\Psi}}+\underline{\underline{\Delta\Psi}}\right)} \left(\varphi_\ell^{(w')}+\Delta\varphi_\ell^{(w')}\right)^2 t'} \delta f_\ell$$

Without loss of generality, we assume $\Delta\varphi_\ell^{(w)} > 0$ and consider two situations of interest:

(*i*) $\varphi_\ell^{(w)} < 0.05 \le \varphi_\ell^{(w)} + \Delta\varphi_\ell^{(w)}$: $\delta t^{(w)}\left(\underline{\underline{\Psi}}\right) = 0$, the error $\delta t^{(w)}\left(\underline{\underline{\Psi}}+\underline{\underline{\Delta\Psi}}\right) - \delta t^{(w)}\left(\underline{\underline{\Psi}}\right) = \delta t^{(w)}\left(\underline{\underline{\Psi}}+\underline{\underline{\Delta\Psi}}\right)$ is typically small since both $\varphi_\ell^{(w)}$ and $\Delta\varphi_\ell^{(w)}$ are small

(*ii*) $\varphi_\ell^{(w)} \ge 0.05, \varphi_\ell^{(w)} + \Delta\varphi_\ell^{(w)} \ge 0.05$: the error

$$\delta t^{(w)}\left(\underline{\underline{\Psi}}+\underline{\underline{\Delta\Psi}}\right) - \delta t^{(w)}\left(\underline{\underline{\Psi}}\right) \approx \frac{\Delta\varphi_\ell^{(w)} t}{\sum_{w' \in \hat{\mathcal{W}}\left(\underline{\underline{\Psi}}\right)} \left(\varphi_\ell^{(w')}\right)^2 t'} \delta f_\ell$$

is also small since $\Delta\varphi_\ell^{(w)} t << \sum_{w' \in \hat{\mathcal{W}}\left(\underline{\underline{\Psi}}\right)} \left(\varphi_\ell^{(w')}\right)^2 t'$

Therefore, the impact of the errors in the *PTDF*s on the *TLR* curtailment quantity is bounded by a small quantity. Notice that the 0.05 threshold helps reduce the impact of the errors in *PTDF*s by excluding *I-W* node pairs with small-valued *PTDF*s which are typically associated with more pronounced relative errors.

In this section, we analytically determined the bounds on the relative errors in the evaluation of *UTC* and *TLR* activities. The error bounds indicate that these impacts are minor.

5 SIMULATION RESULTS

To investigate the quality and robustness of the distribution factor approximations for congestion modeling, we have simulated various cases on a number of test systems including the IEEE 118-bus system and portions of the Eastern Interconnection of the United States. Our simulations indicate that the errors of the approximations stay in an acceptable range under a broad spectrum of conditions. In this section, we summarize representative results of our studies.

We focus our discussion on three sets of representative network conditions: (*a*) the base case condition; (*b*) the 50% reactance cases where, for a set of specified lines, we decrease by 50% the reactance of each line individually; and (*c*) the line outage cases where each line in the same set is outaged individually.

We use the AC power flow results for benchmark purposes and use the absolute value of the relative error as the metric in our assessment. Let y_{true} be the quantity computed using the AC power flow and y be the result obtained using the distribution factors, then the absolute value of the relative error,

$$\varepsilon_y \triangleq \left| \left(y - y_{true}\right) / y_{true} \right| \tag{25}$$

is a unit free quantity. We henceforth refer to ε_y as simply the relative error. The relative errors of interest are those associated with the active line flows to evaluate the overall quality of the distribution factor approximations. In addition, we evaluate the relative errors in the *UTC* quantities and the *TLR* curtailments in the *ATC* and *TLR* studies, respectively.

We discuss first the quality of the *ISF* approximations in evaluating the active line flow changes due to changes in nodal injections under various conditions. We use the *ISF* values of the base case for all the cases studied. For the base case condition (*a*), we study the approximation with different values of injections at a set of specified buses. We vary the injection in step of 10% from 0 to 200% of the base case value for each bus in the set and evaluate the active power flow changes on all the lines using the *ISF* expression. This sensitivity study is repeated for every bus in the set. We collect the relative errors in these results and evaluate their density distribution. The resulting plot is shown in Figure 1(*a*). We perform the same study for every case in the set for (*b*) and (*c*). We collect the relative errors of all the cases for the respective set and plot their distribution density in Figure 1(*b*) and (*c*), respectively. We also display in Figure 2 the cumulative distributions of the relative errors for these cases.

Each of the density plots shows that the frequency for the relative errors is high for small values and very low for large values in each of the cases studied. The cumulative plot makes clear that the base case *ISF* values hold over a wide range of conditions including contingencies. In fact, the scatter plot in Figure 3, showing the

size of relative error as a function of the magnitude of the corresponding *ISF*, further enforces the notion that large errors in *ISF* approximations are associated primarily with the small magnitude *ISF*s. The plots in Figure 1-3 are representative of the results we obtained with the different systems studied.

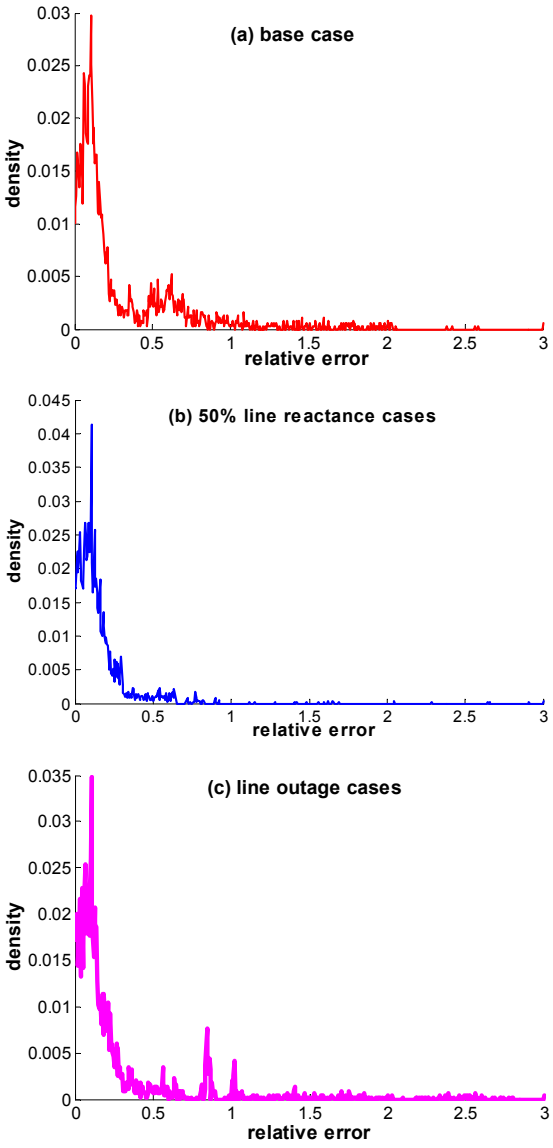

Figure 1: Error distribution of ISF line flow approximations.

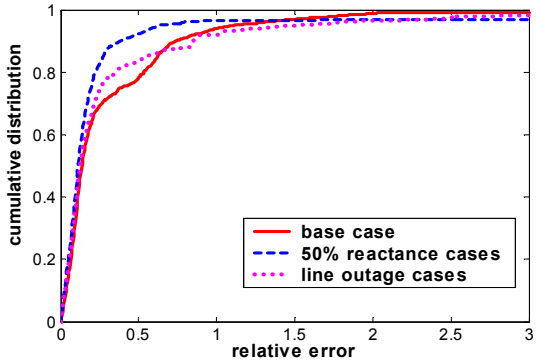

Figure 2: Cumulative distribution of the relative errors.

We next assess the errors in the *UTC* calculations. A similar study is performed in computing the *UTC* values determined using the base case *PTDF*s with respect to those using the AC power flow for the cases (*a*), (*b*) and (*c*). We collect the errors for each of these cases and compute the distribution density of these errors. Figure 4 shows the cumulative distribution of the relative errors for these three cases. The plots indicate that, ignoring the impacts of the changes in the network parameters and topology on the *PTDF*s results in the errors of the *UTC* values that stay in an acceptable range over a wide spectrum of conditions.

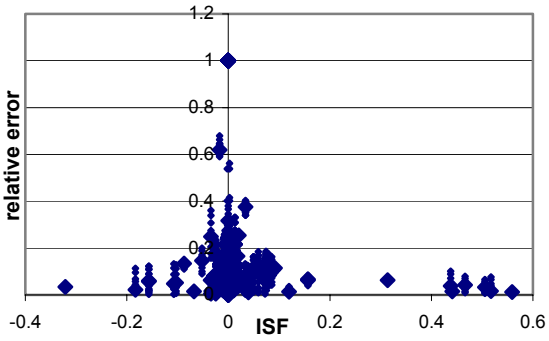

Figure 3: Relationship of relative errors and *ISF*s

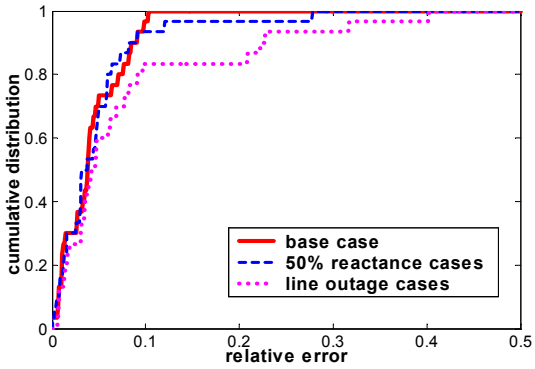

Figure 4: Cumulative error distribution of *UTC* approximation

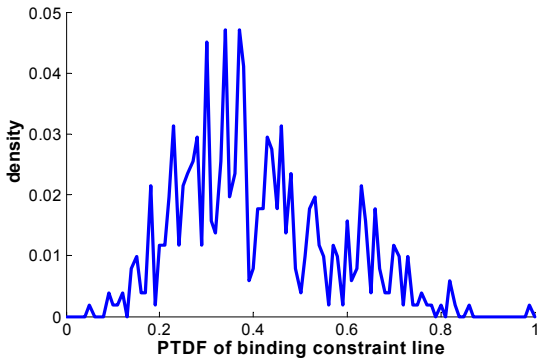

Figure 5: Distribution of *PTDF*s of binding constraint lines

We display in Figure 5 the distribution density of the *PTDF* values of the binding constraint lines in the *UTC* calculations. The plot indicates that the binding constraint lines that determine the *UTC* quantities are typically associated with large-valued *PTDF*s. This result is particularly important considering the analytical bounds derived in section 4. The analytical bounds derived for the *UTC* evaluations depend on the relative errors in the *PTDF*s associated with the binding constraint lines and

the relative errors associated with large-valued *PTDF*s are typically small. Consequently, the analytical bounds determined in section 4 are small.

We also study the impacts of the *PTDF* errors on the *TLR* curtailment quantities. We consider a set of congestions for each case in (*b*) and (*c*). We compute the *TLR* curtailment quantities using the base case *PTDF*s and compare them with the corresponding curtailment quantities computed using the *PTDF*s associated with the modified network. We collect the errors and plot the distribution density of the absolute errors for the cases in (*b*) and (*c*) in Figure 6.

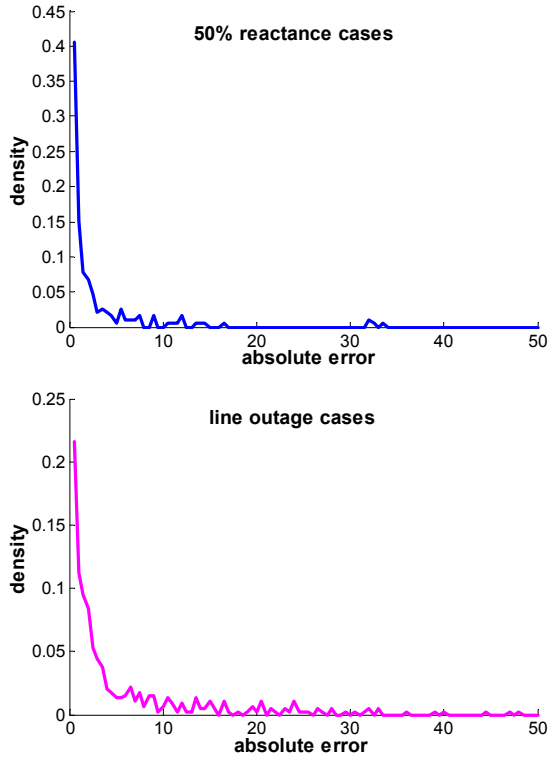

Figure 6: Error distribution of *TLR* curtailment

Figure 6 indicates that the errors in the *PTDF*s have very limited impact on the *TLR* curtailment quantities in both cases.

6 CONCLUSION

We reported on our investigation in the robustness and quality of approximations provided by key distribution factors such as *ISF* and *PTDF*. We examined the range of conditions over which these factors can provide a reliable approximation for large power system networks. This constitutes the first effort to systematically assess the impacts of errors in the distribution factors in the area of congestion modeling. Numerical results indicate that the errors of the approximations stay in an acceptable range under a broad spectrum of conditions including contingencies used to establish *n-1 security*. An attractive characteristic is that larger errors are typically associated with the small-valued *PTDF*s and these errors fail to affect the overall results in either *ATC* or *TLR* calculations. We will report the role of these factors in the definition and implementation of the financial transmission rights (*FTR*s) and flowgate rights (*FGR*s) in a future paper.

ACKNOWLEDGMENT

The research reported here was performed under the sponsorship of PSERC, CERTS and NSF.

REFERENCES

[1] Transmission Transfer Capability Task Force, "Available Transfer Capability Definitions and Determination", North American Electric Reliability Council, Princeton, New Jersey, June 1996

[2] North American Electric Reliability Council, "Appendix 9C – Transmission Loading Relief Procedure", www.nerc.com

[3] W. Hogan, "Contract Networks for Electric Power Transmission", Journal of Regulatory Economics, Vol. 4, 1992, pp. 211-242

[4] H. Chao and S. Peck, "A Market Mechanism for Electric Power Transmission", Journal of Regulatory Economics, Vol. 10, 1996, pp. 25-59

[5] A. Wood and B. Wollenberg, "Power Generation Operation and Control", New York, John Wiley & Sons, ISBN 0-471-58699-4, pp. 105-108

[6] G. Gross and S. Tao, "A physical-flow-based approach to allocating transmission losses in a transaction framework", IEEE Transactions on Power Systems. Vol. 15 n. 2 May 2000, pp. 631-637

[7] L. Chua and P. Lin, "Computer-Aided Analysis of Electronic Circuits: Algorithms & Computational Techniques", Englewood Cliffs, Prentice-Hall, ISBN 0-13-165415-2, pp.134-140

[8] G. Golub and C. Loan, "Matrix Computations", Baltimore, The John Hopkins University Press, ISBN 0-8018-3772-3, pp. 49-53

[9] Transmission Transfer Capability Task Force, "Transmission Transfer Capability", North American Electric Reliability Council, Princeton, New Jersey, May 1995